

gauze-covered openings. As soon as the corals were submerged again, the openings were closed and, for exactly 3 min, a water current equivalent to ambient currents was generated by an electric pump, causing the detachment of mucus from the corals. We then removed the corals and thoroughly mixed the water before collecting samples (50–150 ml, $n = 3$ for each analysis) from all six containers for dry mass, POC and PN analysis.

Mucus production of fully submerged colonies of *A. millepora* and *A. aspera* was quantified as described²⁶. In brief, the small *Acropora* colonies ($n = 8$ in each of two independent experiments) were carefully transferred into sea water-filled glass beakers (500–2,000 ml) and incubated separately for 4–6 h under *in situ* conditions. Three additional beakers without coral and with unfiltered sea water were incubated as controls. At the end of the incubation time, the corals were removed from the glass beakers and the remaining water was mixed. Water samples from each of the eight beakers were taken for dry mass, carbon and nitrogen determination as described above. The results of all experiments were related to the three-dimensional surface area of the coral branches, which was assessed by a wax-coating method²⁷.

Daily mucus release of *Acropora* corals per m² of reef was calculated by using a factor of 3.8 to recalculate the three-dimensional surface area of the corals to the two-dimensional reef rim area covered by *Acropora*. This recalculation factor was derived from the ratio of measured coral surface area to the two-dimensional area (length × width) of the same coral colonies ($n = 15$). We calculated the coral-covered area on the Heron Island Reef rim from a satellite picture (Fig. 2a).

Hard coral coverage

Spatial distributions of hard corals on the reef rim were determined along nine randomly placed line transects. A counting grid (1 m²) was moved ten times along each line transect (10 m in length). Hard corals were identified down to species level, permitting calculation of the percentage cover of *Acropora*.

Oxygen consumption in suspended mucus

Freshly collected *Acropora* mucus and separately ambient sea water were incubated in 30-ml bottles in the dark and at *in situ* temperature (26–29 °C). Incubations started within 60 min of mucus collection or, if this was not possible, coral mucus was kept at 4 °C until incubation. We measured the O₂ concentrations in the incubated solutions simultaneously in time series by the Winkler titration method, and derived O₂ consumption rates from linear regression with at least four data points. Measurements were repeated on five different mucus samplings.

Water level measurements

Tide-induced water level differences between the lagoon and the water surrounding the Heron Reef were measured with a hydraulic potentiometer during two spring low tides.

In situ benthic chamber incubations

We studied benthic degradation of coral mucus in four independent *in situ* incubations using stirred advection chambers similar to those described in ref. 28. Details of these chamber experiments are found in ref. 20 and in the Supplementary Information.

Received 6 October 2003; accepted 15 January 2004; doi:10.1038/nature02344.

- Goreau, T. F., Goreau, N. I. & Goreau, T. J. Corals and coral reefs. *Sci. Am.* **241**, 124–135 (1979).
- Crossland, C., Barnes, D. & Borowitzka, M. Diurnal lipid and mucus production in the staghorn coral *Acropora acuminata*. *Mar. Biol.* **60**, 81–90 (1980).
- Davies, P. S. The role of zooxanthellae in the nutritional energy requirements of *Pocillopora eydouxi*. *Coral Reefs* **2**, 181–186 (1984).
- Muscatine, L., McCloskey, L. R. & Marian, R. E. Estimating the daily contribution of carbon from zooxanthellae to coral animal respiration. *Limnol. Oceanogr.* **26**, 601–611 (1981).
- Meikle, P., Richards, G. & Yellowless, D. Structural investigations on the mucus from 6 species of coral. *Mar. Biol.* **99**, 187–193 (1988).
- Ducklow, H. & Mitchell, R. Bacterial populations and adaptations in the mucus layers on living corals. *Limnol. Oceanogr.* **24**, 715–725 (1979).
- Krupp, D. A. Mucus production by corals exposed during an extreme low tide. *Pacif. Sci.* **38**, 1–11 (1984).
- Schuhmacher, H. *Proc. 3rd Int. Coral Reef Symp. Miami, Florida* 503–509 (University of Miami, Florida, 1977).
- Coles, S. & Strathman, R. Observations on coral mucus flocs and their potential trophic significance. *Limnol. Oceanogr.* **18**, 673–678 (1973).
- Marshall, M. Observations on organic aggregates in the vicinity of coral reefs. *Mar. Biol.* **2**, 50–55 (1968).
- Johannes, R. Ecology of organic aggregates in the vicinity of a coral reef. *Limnol. Oceanogr.* **12**, 189–195 (1967).
- Romaine, S., Tambutte, E., Allemand, D. & Gattuso, J. P. Photosynthesis, respiration and calcification of a zooxanthellate scleractinian coral under submerged and exposed conditions. *Mar. Biol.* **129**, 175–182 (1997).
- Moriarty, D. J. W., Pollard, P. C. & Hunt, W. G. Temporal and spatial variation in bacterial production in the water column over a coral reef. *Mar. Biol.* **85**, 285–292 (1985).
- Ferrier-Pages, C., Leclercq, N., Jaubert, J. & Pelegri, S. P. Enhancement of pico- and nanoplankton growth by coral exudates. *Aquat. Microb. Ecol.* **21**, 203–209 (2000).
- Vacelet, E. & Thomassin, B. Microbial utilization of coral mucus in long term *in situ* incubation over a coral reef. *Hydrobiologia* **211**, 19–32 (1991).
- Shanks, A. L. & Edmondson, E. W. Laboratory-made artificial marine snow—a biological model of the real thing. *Mar. Biol.* **101**, 463–470 (1989).
- Riedl, R. J., Huang, N. & Machan, R. The subtidal pump: a mechanism of interstitial water exchange by wave action. *Mar. Biol.* **13**, 210–221 (1972).
- Parnell, K. E. Water movement within a fringing reef flat, Orpheus Island, North Queensland, Australia. *Coral Reefs* **5**, 1–6 (1986).

- Oberdorfer, J. A. & Buddemeier, R. W. Coral-reef hydrology: field studies of water movement within a barrier reef. *Coral Reefs* **5**, 7–12 (1986).
- Wild, C. *et al.* Degradation and mineralization of coral mucus in reef environments. *Mar. Ecol. Prog. Ser.* **267**, 159–171 (2004).
- Marsden, J. & Meeuwig, J. Preferences of planktotrophic larvae of the tropical serpulid *Spirobranchus giganteus* (Pallas) for exudates of corals from a Barbados reef. *J. Exp. Mar. Biol. Ecol.* **137**, 97–104 (1990).
- Benson, A. & Muscatine, L. Wax in coral mucus—energy transfer from corals to reef fishes. *Limnol. Oceanogr.* **19**, 810–814 (1974).
- Richman, S., Loya, Y. & Slobodkin, L. Rate of mucus production by corals and its assimilation by the coral reef copepod *Acartia negligens*. *Limnol. Oceanogr.* **20**, 918–923 (1975).
- Wilkinson, C. R. Microbial ecology on a coral reef. *Search* **18**, 31–33 (1987).
- Richter, C., Wunsch, M., Rasheed, M., Kotter, I. & Badran, M. I. Endoscopic exploration of Red Sea coral reefs reveals dense populations of cavity-dwelling sponges. *Nature* **413**, 726–730 (2001).
- Hernld, G. J. & Velimirov, B. Microheterotrophic utilization of mucus released by the Mediterranean coral *Cladocora cespitosa*. *Mar. Biol.* **90**, 363–369 (1986).
- Stimson, J. & Kinzie, R. A. The temporal pattern and rate of release of zooxanthellae from the reef coral *Pocillopora damicornis* (Linnaeus) under nitrogen-enrichment and control conditions. *J. Exp. Mar. Biol. Ecol.* **153**, 63–74 (1991).
- Huettel, M. & Gust, G. Solute release mechanisms from confined sediment cores in stirred benthic chambers and flume flows. *Mar. Ecol. Prog. Ser.* **82**, 187–197 (1992).

Supplementary Information accompanies the paper on www.nature.com/nature.

Acknowledgements We thank M. Alisch, S. Menger, H. Woyt, S. Gonelli and L. Hönemann for experimental assistance and for help with chemical analyses; O. Hoegh-Guldberg, R. Johnstone, T. Upton, R. Forbes and other staff members of Heron Island Research Station for logistical assistance; and P. Cook, C. Richter, R. Tollrian and H. Zech for improving the manuscript. All sample collections and *in situ* experiments were carried out under permits issued by the Great Barrier Reef Marine Park Authority. The Max Planck Society, Germany, funded this research.

Authors' contributions M.H. and C.W. conceptually designed and coordinated all experimental work, made most of the measurements, and wrote the manuscript. A.K. quantified coral distribution on Heron Island. S.K. and M.R. helped with chamber experiments and water analyses. B.B.J. contributed with ideas and advice to the significant improvement of the manuscript.

Competing interests statement The authors declare that they have no competing financial interests.

Correspondence and requests for materials should be addressed to C.W. (cwild@mpi-bremen.de).

Optimal traffic organization in ants under crowded conditions

Audrey Dussutour^{1,2}, Vincent Fourcassie¹, Dirk Helbing³ & Jean-Louis Deneubourg²

¹Centre de Recherches sur la Cognition Animale, UMR CNRS 5169, Université Paul Sabatier, 118 Route de Narbonne, F-31062 Toulouse Cedex 4, France

²Centre d'Études des Phénomènes Non-linéaires et des Systèmes Complexe, Université Libre de Bruxelles, CP231, Boulevard du Triomphe, 1050 Bruxelles, Belgium

³Institute for Economics and Traffic, Dresden University of Technology, D-01062 Dresden, Germany

Efficient transportation, a hot topic in nonlinear science¹, is essential for modern societies and the survival of biological species. Biological evolution has generated a rich variety of successful solutions², which have inspired engineers to design optimized artificial systems^{3,4}. Foraging ants, for example, form attractive trails that support the exploitation of initially unknown food sources in almost the minimum possible time^{5,6}. However, can this strategy cope with bottleneck situations, when interactions cause delays that reduce the overall flow? Here, we present an experimental study of ants confronted with two alternative routes. We find that pheromone-based attraction generates one trail at low densities, whereas at a high level of crowding, another trail is established before traffic volume is affected, which guarantees that an optimal rate of food return is maintained. This bifurcation phenomenon is explained by a

nonlinear modelling approach. Surprisingly, the underlying mechanism is based on inhibitory interactions. It points to capacity reserves, a limitation of the density-induced speed reduction, and a sufficient pheromone concentration for reliable trail perception. The balancing mechanism between cohesive and dispersive forces appears to be generic in natural, urban and transportation systems.

Animals living in groups^{7,8} often display collective movement along well-defined lanes or trails^{9–13}. This behaviour emerges through self-organization resulting from the action of individuals on the environment^{14–16}. In ants^{17,18}, for example, mass recruitment allows a colony to make adaptive choices based solely on information collected at the local level by individual workers. When a scout ant discovers a food source, it lays an odour trail on its way back to the nest. Recruited ants use the trail to find the food source and reinforce it in turn on their way back to the nest. Without significant crowding, mass recruitment generally leads to the use of only one trail¹⁹, because small initial differences in pheromone concentration between the trails are amplified as greater numbers of ants choose the trail that was initially slightly stronger, and hence reinforce it. This, together with travel time, ant numbers and ant individual behaviours, also explains why ants use the shortest among several paths leading to the same food source^{19,20}.

Here, we investigate the regulation of traffic flow during mass recruitment in the black garden ant *Lasius niger*. Ants were forced to move on a diamond-shaped bridge that formed two branches between their nest and a food source (Fig. 1). We studied to what extent the traffic on the bridge remains asymmetrical (and therefore limited by the capacity of one branch) when an increased level of crowding is induced by using branches of reduced width ($w = 10.0, 6.0, 3.0$ and 1.5 mm). The temporal evolution of the flow of ants on the bridge shown in Fig. 2 is typical of a trail recruitment process²¹. Surprisingly, the recruitment dynamics was not influenced by the branch width w and the traffic volumes were the same (analysis of variance, ANOVA, $F_{3,44} = 0.500, P = 0.690$). However, for $w = 10$ mm, the majority of ants used the same branch (Fig. 3a), whereas for $w \leq 6$ mm most experiments led to symmetrical traffic ($\chi_2 = 1.686, \text{d.f.} = 2, P = 0.430$). This suggests that there is a transition from asymmetrical to symmetrical traffic between 10.0 and 6.0 mm ($\chi_2 = 12.667, \text{d.f.} = 3, P = 0.005$).

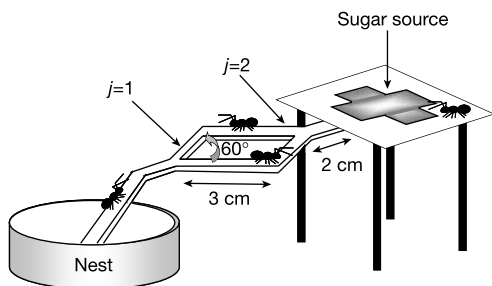


Figure 1 Experimental set-up. Five queenless colonies of *L. niger* (Hymenoptera, Formicidae), each containing 500 workers, were used. During an experiment, ants had access from the nest to a source of food (2 ml of 1 M sucrose solution) placed at the end of a diamond-shaped bridge. The solution was spread over a large surface so that all ants arriving at the end of the bridge could have access to the food. $j = 1$ and $j = 2$ indicate the choice points for branch selection. The whole set-up was surrounded by white curtains to prevent any bias in branch choice caused by the use of visual cues. The colonies were starved for four days before each experiment. The traffic on the two-branch bridge was recorded by a video camera for one hour. Nestbound and outbound ants were then counted and aggregated over 1-min intervals. Counting began as soon as the first ant climbed the bridge. Four different bridge widths (w) were used. This set-up mimics many natural situations in which the geometry of the trails is influenced by physical constraints of the environment, such as the diameter of underground galleries or of the branches in the vegetation along which the ants are moving.

We have identified the mechanism for this ‘symmetry-restoring transition’ using experiments, analytical calculations and Monte Carlo simulations. Figure 3b shows that the proportion of experiments producing symmetrical flows on narrow bridges increases with the total number of ants crossing the bridge ($\chi_2 = 4.6, \text{d.f.} = 2, P = 0.04$). Moreover, Fig. 3c shows that both branches were equally used by the opposite flow directions. Therefore, in contrast to army ants⁶ and pedestrians¹, separation of the opposite flow directions was not found. This could be explained by a high level of disturbance, such as a large variation in the speeds of ants²².

The flow of ants over the bridge can be understood analytically. The concentration of the trail pheromone C_{ij} on branch i ($i = 1, 2$) immediately behind each choice point j ($j = 1, 2$) changes in time t according to:

$$dC_{ij}/dt = q\Phi_{ij}(t) + q\Phi_{ij'}(t - \tau) - \nu C_{ij}(t) \text{ with } j' = 3 - j \quad (1)$$

where $\Phi_{i1}(t)$ represents the overall flow of foragers from the nest to the food source that choose branch i behind the choice point 1, $\Phi_{i2}(t)$ is the opposite flow on branch i behind the other choice point $j' = 3 - j = 2$, τ is the average time required for an ant to get from one choice point to the other, q is the quantity of pheromone laid on the trail, and ν is the decay rate of the pheromone. Moreover, if the density is low enough:

$$\Phi_{ij}(t) = \phi_j(t)F_{ij}(t) \quad (2)$$

where ϕ_1 is the outbound flow of foragers from the nest to the food source and ϕ_2 is the opposite, nestbound flow. The function F_{ij} describes the relative attractiveness of the trail on branch i at choice point j . For *L. niger* it is given by¹⁹:

$$F_{ij} = \frac{(k + C_{ij})^2}{(k + C_{1j})^2 + (k + C_{2j})^2} = 1 - F_{i'j} \text{ with } i' = 3 - i \quad (3)$$

where k denotes a concentration threshold beyond which the pheromone-based choice of a trail begins to be effective.

Equation (2) describes the flow dynamics without interactions between ants. However, when traffic was dense, we observed that ants that had just started to move on one branch were often pushed to the other branch, having collided frontally with another ant coming from the opposite direction. This behaviour will turn out to be essential in generating symmetrical traffic on narrow bridges.

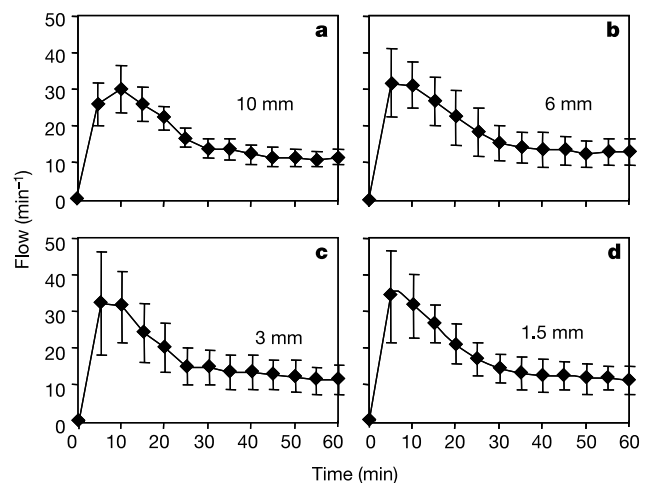


Figure 2 Average number of ants per minute crossing the two branches of the bridge within intervals of five minutes. The observed traffic volumes $2\phi(t)$ and flow dynamics agreed for the four different branch widths, that is, the bottleneck for smaller branches was compensated for by use of both branches. **a**, $w = 10$ mm; **b**, $w = 6$ mm; **c**, $w = 3$ mm; **d**, $w = 1.5$ mm. $N = 12$ experiments were carried out for each bridge width. Error bars indicate the standard deviation.

Whereas pushing was practically never observed on a 10-mm bridge, on narrow bridges the frequency of pushing events was high and proportional to the flow (Fig. 3d).

When pushing is taken into account, the overall flow of ants arriving at choice point j and choosing branch i can be expressed by the following formula:

$$\Phi_{ij}(t) = \phi_j(t)F_{ij}(t)[1 - \gamma a \Phi_{ij'}(t - \tau)/w] + \phi_j(t)F_{i'j}(t)\gamma a \Phi_{ij'}(t - \tau)/w \quad (4)$$

The first term on the right-hand side of equation (4) represents the flow of ants engaged on branch i (that is, $\phi_j(t)F_{ij}(t)$), diminished by the flow of ants pushed towards the other branch i' by ants arriving from the opposite direction. $a\Phi_{ij'}(t - \tau)/w$ is the proportion of ants decelerated by interactions. The factor a is proportional to the interaction time period and the lateral width of ants. Up to the symmetry-restoring transition it can be considered approximately constant. $\gamma \approx 0.57$ denotes the probability of being pushed in the case of an encounter (Fig. 3d). The second term on the

right-hand side of equation (4) represents the flow of ants that were engaged on branch i' and were pushed towards branch i .

The stationary solutions of this model are defined by the conditions $dC_{ij}/dt = 0$, $F_{ij}(t - \tau) = F_{ij}(t) = F_{ij}$, $\Phi_{ij}(t - \tau) = \Phi_{ij}(t) = \Phi_{ij}$ and $\phi_j(t - \tau) = \phi_j(t) = \phi_j' = \phi$ (because the nest-bound flow and the outbound flow should be equal). These imply:

$$C_{ij} = q(\Phi_{ij} + \Phi_{ij'})/\nu = C_{ij'} \quad F_{ij} = F_{ij'} = 1 - F_{i'j} = 1 - F_{i'j'}$$

and

$$C_{ij} = C_{ij'} = \frac{q\phi}{\nu} + D, \quad C_{i'j} = C_{i'j'} = \frac{q\phi}{\nu} - D \quad (5)$$

with

$$D = 0 \quad (6)$$

or

$$D^2 = \frac{q^2\phi^2}{\nu^2} - \frac{k^2 + \gamma a \phi(k + 2q\phi/\nu)^2/w}{1 + \gamma a \phi/w} \quad (7)$$

We can distinguish two cases. Case (1): when $D^2 > 0$, the stable

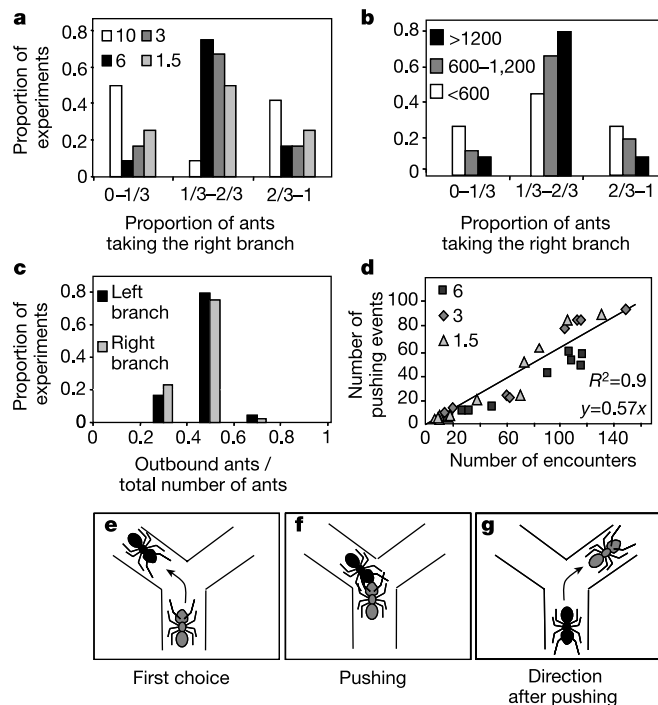


Figure 3 Experimental results. **a**, Experimental frequency distributions of the proportion F_{1j} of ants using the right branch for different branch widths. We considered traffic to be asymmetrical when more than 2/3 of the cumulated traffic of ants at the end of the experiment had used a single branch. All experiments have been pooled. **b**, Experimental frequency distributions similar to **a**, but for different total numbers of ants crossing the bridge. All experiments on bridges of $w = 1.5, 3.0$ and 6.0 mm have been pooled. **c**, Proportion of outbound ants on the left and right branches of the bridge divided by the total number of ants that have passed the bridge at the end of the experiment. The results contradict opposite one-way flows on both branches. **d**, Number of pushing events as a function of the total number of ant encounters on the initial part of each branch of the bridge. For each branch width, pushing events were evaluated at both choice points, for outbound and nestbound ants, during the first ten and last ten minutes of a random sample of two experiments characterized by symmetrical and two experiments characterized by asymmetrical traffic. This yielded a total of 2 branches \times 4 experiments \times 2 time intervals = 16 points per branch width. When the number of encounters was too low (≤ 3) the points were not taken into account in the regression. The slope of the linear regression is equal to 0.571 ± 0.057 (confidence interval, $CI_{95\%}$). This corresponds to the probability γ that an ant will be pushed and redirected towards the other branch after encountering another ant coming from the opposite direction (see **e-g**).

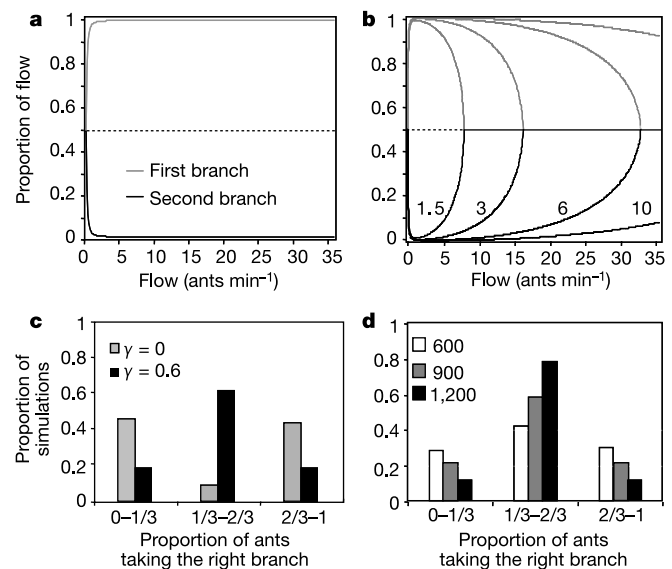


Figure 4 Analytical and Monte Carlo simulation results. **a, b**, Analytical results for the parameter values $q = 1$, $k = 6$, $\nu = 1/40 \text{ min}^{-1}$, and $a = 0.1 \text{ mm min}$, which have been adjusted to experimental measurements. The curves show the proportion F_{ij} of the overall flow ϕ on each branch in the stationary state. **a**, In the absence of pushing ($\gamma = 0$) the model predicts asymmetrical traffic above very low values of the overall flow of ants, independently of the traffic volume. **b**, When the proportion of pushed ants is high ($\gamma = 0.6$), traffic is asymmetrical for moderate values of the overall flow of ants, but stable symmetrical traffic with $F_{ij} = 0.5$ is expected above a critical value of traffic flow, which is an increasing function of branch width. The symmetry-restoring transition from asymmetrical to symmetrical traffic flow corresponds to an inverse pitchfork bifurcation. **c, d**, Results of Monte Carlo simulations. At time $t = 0$, the pheromone concentration and the number of ants on each branch are set to zero. Ants arrive at choice point j at a rate $\phi_j(t) = \phi$. The probability of choosing the right or left branch at a choice point is governed by the choice function F_{ij} (see equation (3)). However, as soon as an ant has engaged on a branch, it may be pushed to the other branch with probability γ by an ant moving in the opposite direction coming from the second choice point. The pushed ant then continues its course on the alternative branch and lays a trail. For each value of γ , the simulations are averaged over 1,000 runs. The graphs show the relative frequency of simulations in which a certain proportion of traffic was supported by the right branch. **c**, Assuming a pushing probability equal to zero ($\gamma = 0$), most simulations ended with asymmetrical traffic. However, when we used the experimental value $\gamma = 0.6$, most simulations for narrow branches resulted in symmetrical traffic. **d**, The proportion of simulations with $\gamma = 0.6$ in which asymmetrical traffic emerged is a function of the total number of ants crossing the bridge, just as in our experiments (compare Fig. 3b).

stationary solution corresponds to asymmetrical traffic with $C_{ij} = \frac{q\phi}{v} \pm \sqrt{D^2}$ and $C_{ij} = \frac{q\phi}{v} \mp \sqrt{D^2}$. If $\gamma = 0$, this situation is given for $q\phi/v > k$. If $q\phi/v \leq k$, that is, if the pheromone concentration is too low, the ants choose both branches at random, corresponding to a symmetrical distribution (Fig. 4a). Case (2): when pushing is taken into account with $\gamma > 0$, the organization of traffic changes considerably: the asymmetrical solution can no longer be established as soon as $D^2 < 0$ for large traffic volumes ϕ (Fig. 4b). In this case, symmetrical traffic is expected with $C_{ij} = q\phi/v$ and $\Phi_{ij} = \phi/2$ for both branches i and choice points j . Therefore, high traffic volumes can be maintained and none of the branches is preferred in spite of the competitive effect due to the accumulation of pheromone on both branches. Moreover, the model implies that the outbound flow Φ_{i1} and the nestbound flow Φ_{i2} are equal, indicating that one-way flows are not required to maintain a high traffic volume²³. These analytical results have been confirmed by Monte Carlo simulations (see Fig. 4c, d). Our simulations have also demonstrated that if pushed ants, instead of moving to the other branch, made a U-turn and returned in the direction they had been coming from, the overall flow of ants crossing the bridge was affected by the branch width and no shift to symmetrical traffic was observed.

The traffic organization in ants can be called optimal. The overall flow on branch i behind choice point j is given by $\Phi_{ij} = w\rho_{ij}V_{ij} \leq \phi$, where ρ_{ij} denotes the density of ants. Their average speed is theoretically estimated by $V_{ij} \approx V_m(1 - a\Phi_{ij}/w)$, where V_m denotes the average maximum speed and $a\Phi_{ij}/w$ is again the proportion of decelerated ants. For the symmetry-restoring transition with $D^2 = 0$, equation (7) requires $a\gamma\phi/w < 1/3$, which implies $V_{ij} > V_m[1 - 1/(3\gamma)] \approx 0.42V_m$. However, according to the empirical speed–density relation by Burd *et al.*²³, the maximum flow (the capacity) is only reached at the smaller speed $V_{ij} = V_m[1 - 1/(n + 1)] \approx 0.39V_m$. Although the empirical value $n \approx 0.64$ was determined for another ant species, the values for *L. niger* should be comparable. This shows that the symmetry-restoring transition occurs before the maximum flow is reached. The strict inequality also implies capacity reserves and a limitation of the density-related speed reduction. A marginal reduction in speed, however, would not favour symmetrical traffic because of the benefits of using a single trail. First, a more concentrated trail provides a better orientation guidance and a stronger arousal stimulus²⁴. Second, a higher density of ants enhances information exchange and supports a better group defence²⁵.

We have demonstrated the surprising functionality of collisions among ants to keep up the desired flow level by generation of symmetrical traffic. Pushing behaviour may be considered an optimal behaviour to maintain a high rate of food return to the nest. It would not be required in most models of ideal free distribution (IDF)²⁶, as they neglect effects of inter-attraction. The balancing between cohesive and dispersive forces avoids a dysfunctional degree of aggregation and supports an optimal accessibility of space at minimal costs allowing an efficient construction, maintenance and use of infrastructures. This mechanism appears to be generic in nature, in particular in group-living organisms. For example, inhibitory interactions at overcrowded building sites in termites allow a smooth growth of the nest structure²⁷. In the development of urban agglomerations such interactions help to maintain the coexistence of distinct cities²⁸, and in vehicle traffic they determine the choice of longer, less congested routes. The mechanism also suggests algorithms for the routing of data traffic in networks. □

Received 11 December 2003; accepted 13 January 2004; doi:10.1038/nature02345.

1. Helbing, D. Traffic and related self-driven many-particle systems. *Rev. Mod. Phys.* **73**, 1067–1141 (2001).
2. Camazine, S., *et al.* *Self-organized Biological Systems* (Princeton Univ. Press, Princeton, 2001).
3. Bonabeau, E., Dorigo, M. & Theraulaz, G. Inspiration for optimization from social insect behaviour. *Nature* **406**, 39–42 (2000).
4. Bonabeau, E., Dorigo, M. & Theraulaz, G. *Swarm Intelligence: From Natural to Artificial Systems* (Oxford Univ. Press, New York, 1999).

5. Burd, M. & Aranwela, N. Head-on encounter rates and walking speed of foragers in leaf-cutting ant traffic. *Insectes Soc.* **50**, 3–8 (2003).
6. Couzin, I. D. & Franks, N. R. Self-organized lane formation and optimized traffic flow in army ants. *Proc. R. Soc. Lond. B* **270**, 139–146 (2003).
7. Parrish, J. K. & Hamner, W. K. *Animal Groups in Three Dimensions* (Cambridge Univ. Press, Cambridge, UK, 1997).
8. Krause, J. & Ruxton, D. *Living in Groups* (Oxford Univ. Press, Oxford, UK, 2002).
9. Galef, B. G. Jr & Buckley, L. L. Using foraging trails by Norway rats. *Anim. Behav.* **51**, 765–771 (1996).
10. Fitzgerald, T. D. *The Tent Caterpillars* (Cornell Univ. Press, Ithaca, NY, 1995).
11. Erlandson, J. & Kostylev, V. Trail following, speed and fractal dimension of movement in a marine prosobranch, *Littorina littorea*, during a mating and a non-mating season. *Mar. Biol.* **122**, 87–94 (1995).
12. Traniello, J. F. A. & Robson, S. K. in *Chemical Ecology of Insects* (eds Cardé, R. T. & Bell, W.) 241–286 (Chapman & Hall, New York, 1995).
13. Miura, T. & Matusmoto, T. Open-air litter foraging in the nasute termite *Longipeditermes longipes* (Isoptera: Termitidae). *J. Insect Behav.* **11**, 179–189 (1988).
14. Helbing, D., Keltsch, J. & Molnár, P. Modelling the evolution of human trail systems. *Nature* **388**, 47–50 (1997).
15. Edelstein-Keshet, L. W., Ermentrout, J. & Bard, G. Trail following in ants: individual properties determine population behaviour. *Behav. Ecol. Sociobiol.* **36**, 119–133 (1995).
16. Schweitzer, F. *Brownian Agents and Active Particles. Collective Dynamics in the Natural and Social Sciences* (Springer, Berlin, 2003).
17. Wilson, E. O. Chemical communication among workers of the fire ant *Solenopsis saevissima* (Fr. Smith). 1. The organization of mass-foraging. *Anim. Behav.* **10**, 134–147 (1962).
18. Hölldobler, B. & Wilson, E. O. *The Ants* 265–279 (The Belknap Press of Harvard Univ. Press, Cambridge, MA, 1990).
19. Beckers, R., Deneubourg, J. L. & Goss, S. Trails and U-turns in the selection of a path by the ant *Lasius niger*. *J. Theor. Biol.* **159**, 397–415 (1992).
20. Goss, S., Aron, S., Deneubourg, J. L. & Pasteels, J. M. Self-organized shortcuts in the Argentine ant. *Naturwissenschaften* **76**, 579–581 (1989).
21. Pasteels, J. M., Deneubourg, J. L. & Goss, S. in *From Individual to Collective Behaviour in Social Insects* (eds Pasteels, J. M. & Deneubourg, J. L.) *Experientia* suppl. Vol. 54, 155–175 (Birkhäuser, Basel, 1987).
22. Helbing, D. & Platkowski, T. Drift- or fluctuation-induced ordering and self-organization in driven many-particle systems. *Europhys. Lett.* **60**, 227–233 (2002).
23. Burd, M. *et al.* Traffic dynamics of the leaf-cutting ant *Atta cephalotes*. *Am. Nat.* **159**, 283–293 (2002).
24. Calenbuhr, V. *et al.* A model for osmotropotactic orientation. II. *J. Theor. Biol.* **158**, 395–407 (1992).
25. Feener, D. H. & Moss, K. A. G. Defense against parasites by hitchhikers in leaf-cutting ants: a quantitative assessment. *Behav. Ecol. Sociobiol.* **49**, 348–356 (1990).
26. Fretwell, S. D. & Lucas, H. L. On territorial behavior and other factors influencing habitat distribution in birds. I. Theoretical development. *Acta Biotheor.* **19**, 16–36 (1970).
27. O’Toole, D. V., Robinson, P. A. & Myerscough, M. R. Self-organized criticality in termite architecture: a role for crowding in ensuring ordered nest expansion. *J. Theor. Biol.* **198**, 305–327 (1999).
28. Fujita, M., Krugman, P. & Venables, A. *The Spatial Economy—Cities, Regions, and International Trade* (MIT Press, Cambridge, MA, 1999).

Acknowledgements We thank G. Theraulaz and all the members of his team ‘Ethology and modelization of collective behaviours’ for discussions and comments on the manuscript. We also thank A. Schadschneider for discussions.

Competing interests statement The authors declare that they have no competing financial interests.

Correspondence and requests for materials should be addressed to A.D. (dussoutou@cict.fr).

Perceiving distance accurately by a directional process of integrating ground information

Bing Wu¹, Teng Leng Ooi² & Zijiang J. He¹

¹Department of Psychological and Brain Sciences, University of Louisville, Louisville, Kentucky 40292, USA

²Department of Basic Sciences, Pennsylvania College of Optometry, 8360 Old York Road, Elkins Park, Pennsylvania 19027, USA

By itself, the absolute distance of an object cannot be accurately judged beyond 2–3 m (refs 1–3). Yet, when it is viewed with reference to a flat terrain, humans accurately judge the absolute distance of the object up to 20 m, an ability that is important for various actions^{4–8}. Here we provide evidence that this is accomplished by integrating local patches of ground information into a global surface reference frame. We first show that restricting an